Oxygen Reduction on Nano-structured Platinum Surfaces in acidic media: Promoting effect of surface steps and ideal response of Pt(111)

Ana M. Gómez–Marín*[,a,b] and Juan M. Feliu*[,a]

[a] *Instituto de Electroquímica, Universidad de Alicante, Apt 99, E-03080 Alicante, Spain, Tel.: +34 965 909 301; fax: +34 965 903 537. Email: juan.feliu@ua.es (J.M. Feliu), ana.gomez@ua.edu.co (AM Gomez).*

[b] *Basic Science Department, Fundación Universitaria Luis Amigó, Transversal 51A #67B-90, Medellín, Colombia.*

Abstract:

In this paper, the role of surface steps on the electrocatalytic activity of Platinum nano-structured surfaces for the oxygen reduction reaction (ORR) in acidic medium is evaluated by using stepped surfaces of structure Pt(S)[n(111)x(111)] with large terraces ($20 \leq n \leq 50$). It is realized that the inclusion of an even low amount of surface steps enhances the ORR, and linear activity trends are measured when currents at constant potential are plotted vs. the step density. As a consequence, an *ideal* ORR curve for a defect-free Pt(111) surface is extrapolated at zero defect density from experimental data and can be compared to that of a *quasi perfect* Pt(111) electrode. It is clearly shown that surface steps promote the electrode activity toward ORR in acid medium. Results are discussed in light of available theoretical and experimental data.

Keywords: Oxygen reduction reaction, Pt single crystals, nanostructures surfaces, reactivity, electrocatalyst.

1. Introduction

Oxygen reduction reaction (ORR) is undoubtedly the most important cathodic process in fuel cells; however, despite many year of intense research, the ORR mechanism still remains elusive. Experimentally, the ORR electrode activity follows a volcano-type correlation when it is plotted as function of the adsorption energy of oxygen atoms to the catalyst surface, ΔG_{Oads}, with the polycrystalline platinum catalyst close to the top [1, 2]. Theoretically, calculations state that pure Pt has a slightly large ΔG_{Oads} to be optimal and that the potential determining step in the ORR mechanism, related with the rate determining step (RDS) in some analysis [3–5], is the removal of adsorbed oxygen, O_{ads}, or adsorbed hydroxide, OH_{ads}, from the catalyst surface [3–5]. Following this idea, catalysts with smaller ΔG_{Oads} would have higher ORR activities than pure Pt, and this principle has been used by several groups as a foundational basis in designing new catalysts [9, 10]. However, because of a scaling relationship between the ΔG_{ads} of O_{ads}, OH_{ads} and OOH_{ads} species, it would not be possible any further improvements in the ORR performance, beyond some optimal values for these adsorption bond strengths [3–8].

A similar theoretical principle has been developed in the case of platinum single crystals. In this sense, it has been predicted that open facets, such as steps, edges and kinks, should provide a negligible contribution to the ORR activity, because they bind O-containing adsorbates more strongly that basal planes, whereas active sites are located upon the terraces, in particular the {111} facet [10–13]. However, although Pt(111) is the most active Pt single crystal in alkaline solutions [14], stepped Pt surfaces are more catalytic than the Pt(111) electrode in acidic solutions [15–17], contrary to

theoretical predictions. This is an interesting point, since the predicted reactivity by calculations deals with a material whose electronic surface charge densities are more negative than those in $HClO_4$, (~12 pH units' difference), and raises the question of whether surface charges are appropriately included in theoretical models.

Differences between theoretical and experimental ORR activities at Pt single crystals in acidic media have been explained either because of a symmetry breaking of the hexagonal overlayer on the (111) facet caused by the steps [13], or due to the existence of specific surface terrace sites on stepped surfaces that bind O-containing species more weakly than Pt(111) [18], related, perhaps, to their surface reconstruction [10], in acid but not in alkaline solutions. Hence, in order to clarify the real role of surface steps in the ORR dynamics, it is necessary to measure the ORR activity at well defined stepped Pt(111) surfaces, structurally stable under acidic electrochemical environments, with a percentage of defects low enough to preserve long range ordering of extended surfaces and minimize the existence of surface sites different to terrace and step sites.

Besides, theoretical chemical models can be considered as perfectly ideal. This means, within the state of the art of calculations, that surfaces have no defects and atoms at the surface correspond to the truncation of an ideal single crystal. This is valid for basal planes as well as for stepped or kinked surfaces. Thus, theoretical predictions should be compared to experiments performed on equally ideal electrode surfaces, *e.g. defect-free* single crystal electrodes. However, experimental surfaces, even the most carefully prepared and characterized, always contain defects at atomic level. Hence, theoretical results are only possible to compare with samples fulfilling some quality criteria [19–22], usually not found in results coming from large commercial materials [23].

In this work, single crystal stepped surfaces from small single crystal beads cut with a precision of 2 minutes of arc [24], are prepared, following the best quality requirements after *in situ* characterization. Afterwards, the ORR on those stepped Pt(S)[*n*(111)x(111)] surfaces, with the longest terrace widths reasonably available, is studied to assess the role of surface steps and to calculate the *ideal* ORR curve for a perfect, defect-free, Pt(111) surface [26]. These surfaces are expected to be the most stable upon potential excursions and have uniform terraces, separated by mono-atomic steps, without faceting or reconstruction, if the appropriate experimental protocol is fulfilled [25, 27]. Incidentally, we can assume that defects migrate to the steps in the electrode pretreatment, leaving defect-free terraces [25]. This is similar to the case of large nano-particles that are single crystals in which defects concentrate on the surfaces [28, 29].

2. Experimental

Electrodes with (111) and stepped surfaces having wide terraces, belonging to the series Pt(S)[*n*(111)x(111)] surface orientation were prepared [24]. The stepped surface with longest terraces corresponds to 50 atomic rows and the deviation angle in the [

repeated at least three times, with consistent results.

As explained elsewhere, ohmic corrections, iR_u, were not necessary under our experimental conditions [32]. The exact magnitude of iR_u depends on several factors: the electrode shapes, the potential profile in the cell, cell geometry, solution conductance. However, in any electrochemical experiment, more important than measuring the absolute value of R_u is to determine if iR_u compensation is needed. A simple strategy usually employed is to record some initial data with and without iR_u compensation. If the shape of the curve significantly changes when iR_u compensation is applied, compensation is required. Figure 1 depicts corrected and uncorrected curves taken under our experimental conditions. As seen, curves from corrected and uncorrected data superimpose and so correcting R_u is not necessary. It is important to mention that iR_u compensation often adds additional noise to the data and, in some cases, can induce a negative global coupling into the system. So, iR_u compensation should be applied only when it is necessary.

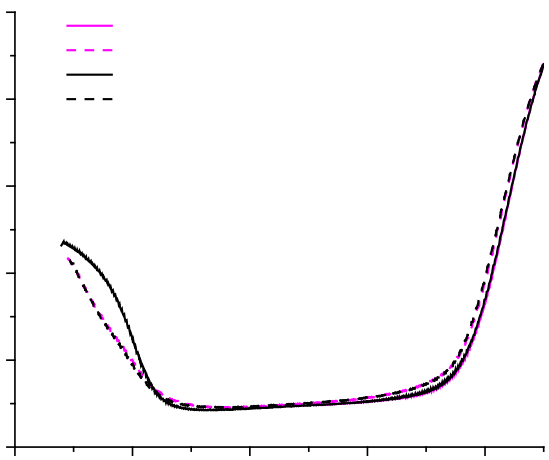

Figure 1: Positive (solid) and negative (dashed) going scans for the ORR on Pt(25 25

24) in oxygen-saturated 0.1 M $HClO_4$ solutions for Ohmic drop corrected (magenta) and uncorrected data (black). Scan rate 50 mV s^{-1}, 1600 rpm.

Results and discussion

Stepped surfaces are characterized by a step orientation, a terrace orientation and a terrace width [27]. For surfaces with terrace widths larger than a few atoms, individual steps are far away enough from each other to consider negligible any interaction between neighbour step dipoles. The Pt(S)[*n*(111)x(111)] series is composed of close-packed {111} terraces, separated at regular intervals by monatomic steps that form {110} micro-facets and a terrace wide equal to *n-1* atoms. In this work *n* = 50, 40, 30, 26 and 20 atoms wide are used, *i.e.* the shortest terrace corresponds to the longest one in reference [16]. Figure 2 shows stable cyclic voltammograms (CVs), in 0.1 M perchloric acid, of Pt(111) and some of the vicinal surfaces employed in this study, while the inset to Fig. 2 depicts a detailed view of the hydrogen adsorption/desorption region for these electrodes.

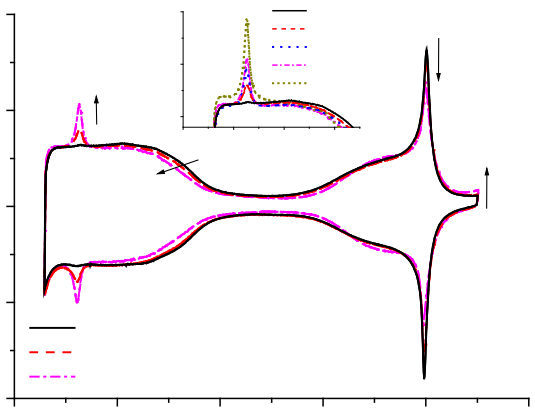

Fig. 2 Stable voltammetric profiles of Pt(111) and stepped surfaces, Pt(S)[*n*(111)x(111)], in 0.1 M $HClO_4$ at 50 mV/s. Inset: Detailed view of the hydrogen adsorption/desorption region.

The CV for Pt(111) and its vicinal surfaces is well established in non-adsorbing electrolytes and can be used as a characteristic fingerprint [27]. On {111} terraces, hydrogen adsorption-desorption, H_{ads}, is responsible for the pseudo-capacitive currents at potentials lower than 0.35 V, whereas the voltammetric charge of the so-called "butterfly" feature, between 0.6 and 0.85 V, has been attributed to the formation of OH_{ads}, from water dissociation [20, 21, 33]. Between these two regions, an apparent double layer region occurs, Fig. 2. On well ordered stepped electrodes, having {111} monatomic steps, a characteristic voltammetric peak appears at 0.13 V, inset to Fig. 2, albeit its origin is not entirely clear. Commonly, it has been attributed to H_{ads} on step sites [27], but its pH dependence suggests possible contributions of OH_{ads} from water dissociation [34]. Increasing the step density linearly increases the charge under this peak, but decreases the H_{ads} and OH_{ads} terrace charges [27].

The ORR was carried out in oxygen-saturated solutions at different rotation rates, ω. Figure 3 collects voltammetric profiles for ORR on some Pt(S)[*n*(111)x(111)] surfaces, between 0 and 0.9 V, at different rotation rates, ω, and a sweep rate of 50 mV s^{-1}. The upper potential limit was selected to assure the surface stability of the stepped surfaces. In addition, because the sweep direction can play an important role in the shape of the CV [16, 19], only the positive going scan is shown. Insets to Fig. 3 depict the plot of the limiting current, j_{lim}, vs. $\omega^{½}$. As can be appreciated, the hydrodynamic response of the system is well described, on each surface, by the standard Levich equation, within reasonable experimental error [15, 16, 19].

Curves on Fig. 3 show similar trends to those already described for Pt(S)[*n*(111)x(111)] surfaces when increasing the step density [16]. In all cases, the j_{lim} is recorded between

~0.30 and 0.70 V. Additionally, as extensively discussed in previous works [15, 16, 19], below E < 0.3 V where H_{ads} is adsorbed, there are two drops in the reduction current. These current drops decrease as the step density increases (for a better detail, see inset to Fig. 7), which suggests that adsorbed hydrogen on terraces, H_{ads}, may prevent O–O bond scission or block surface sites [15, 16, 19]. Therefore only two electrons are exchanged in this potential range.

Fig. 3: Rotating Disk measurements of oxygen reduction on Pt(25 25 24) (A) and Pt(15 15 14), in 0.1 M $HClO_4$ at 50 mV/s. Rotation rates are given on the curves. Insets: Plots of j_{lim} vs. $\omega^{½}$.

To study the ORR kinetics, the kinetic current density, j_k, should be calculated. For a first order reaction, j_k can be expressed as:

According to Eqn. (2), j_k at different potentials can be calculated as the y-axis intercept of the straight lines in Fig. 4. Figure 5 displays values of j_k at different potentials calculated according Eqns. (1) and (2). As can be appreciated, j_k values from both equations give identical results, corroborating that the Levich equation can describe the hydrodynamics of the system. At potentials below 0.75 V, the mass transfer begins to play an important role in the ORR dynamics, and j_k cannot be estimated.

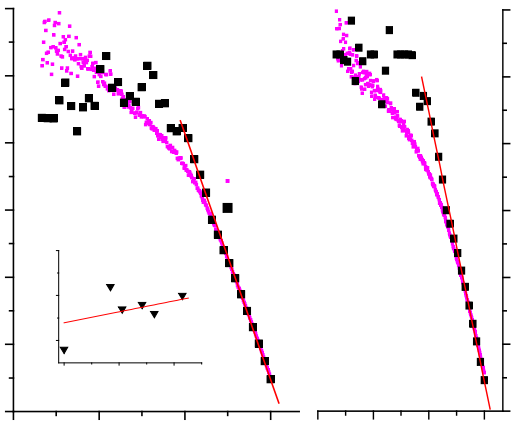

Fig. 5: Log j_k vs. potential calculated for a Pt(25 25 24) (A) and Pt(15 15 14) (B) electrodes in 0.1 M $HClO_4$ at 50 mV/s. Inset: Tafel slope values obtained for ORR reduction on stepped electrodes.

From Fig. 5, Tafel slopes can be determined, see inset. In this work, Tafel slopes from 76 to 82 mV between 0.8 to 0.9 V are calculated for the stepped electrodes [16]. It appears that the Tafel slope systematically varies with the surface order, see inset to Fig. 5A. In the case of Pt(111), experimental Tafel slopes, in this potential region, ranging from 60 to 88 mV have been reported [15, 16, 19]. This experimental dispersion on measured Tafel slopes for Pt(111) could be explained considering that the Tafel slope apparently increases as the step density increases. In consequence, on non well ordered

Pt(111), Tafel slopes would approach those values on stepped electrodes.

The electrocatalytic activity on different single crystals is usually quantified by calculating exchange current density values (j_0) [15]. However, the determination of j_0 for the ORR requires a large extrapolation and so, it is not particularly precise. Alternatively, some reports have used the half-wave potential, $E_{½}$ [16], or the reduction current at some fixed potential [2, 14] for comparing the ORR electrocatalytic activity on different electrodes. Figure 6 shows both approaches: the normalized kinetic current at 0.9 V (Fig. 6A) and $E_{½}$ (Fig. 6B) as function of the electrode step density. It has been shown that $E_{½}$ and j_0 have the same qualitative tendency [16]. It is noteworthy that the experimental responses of our Pt(111) electrode, j/j_{lim} = 0.21 and $E_{½}$ = 0.86 V, are higher than the extrapolated values, despite the high quality of the blank voltammogram. This suggests that all experimental electrodes have certain amount of surface defects. Considering that $j_{lim} \approx 6.0$ mA cm^{-2} at ω = 1600 rpm, so the current density on Pt(111) at 0.9 V is ~1.26 mA cm^{-2}.

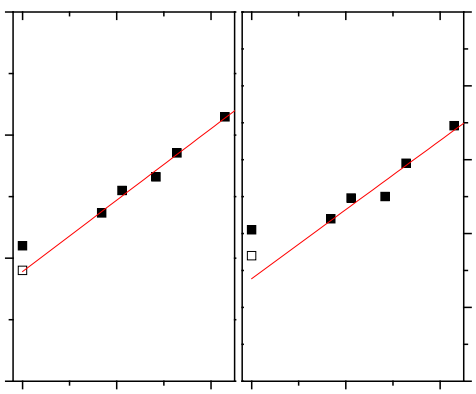

Fig. 6: Plots of the normalized reduction current, j/j_{lim}, at 0.9 V (A) and the half-height potential, $E_{½}$, (B) for the oxygen reduction as a function of the step density at rotation rate of 1600 rpm and 50 mV s^{-1} in 0.1 M $HClO_4$. Empty symbols are extrapolated

values for an *ideal* ORR curve on Pt(111).

From Fig. 6 is clear that the presence of surface steps increases the ORR electrode activity in acid media, despite the higher density of under-coordinated sites on stepped crystals than basal planes, and thus, the enhanced adsorption energy of O_{ads} and OH_{ads}. Similar conclusions were extracted from experimental results on more stepped surfaces [16], as those ones belonging to the series Pt(S)[*n*(110)x(111)] [16], Pt(S)[*n*(111)x (100)] and Pt(S)[*n*(100)x(111)] [15]. Contrarily, as mentioned in the introduction, in alkaline solutions surface steps, irrespectively of its orientation, always have a lower ORR electrode activity than Pt(111) electrodes [14], and so this latter is the most active plane for the ORR.

In consequence, results from this work, do not support the idea about the O_{ads}, or OH_{ads}, removal as the rate determining step for the ORR. Nevertheless, other works have suggested different reasons behind the lack of ORR reduction current for E > 1.0 V [19, 36]. For example, it has been claimed that the reduction of an aqueous intermediate species is the RDS for the reaction [19]. Also, it has been proposed an effective reversible potential for the oxygen four-electron reduction on Pt(111) of ~0.9 V, based on the exergonic O–O bond scission of the adsorbed hydroperoxyl radical OOH_{ads}, being at least 0.9 eV exergonic [36].

When data between the stepped surfaces were compared, it appears that normalized current density values, at constant rotation rate and a fixed potential linearly increase with the step density, Fig 6A. This is also true for E < 0.9 V and so, it is possible to calculate an *ideal* ORR *j*/*E* curve, on a defect-free Pt(111), from the intercept of similar linear plots to Fig 6A but at different potentials, to the value corresponding to a zero

step density condition, n= ∞. For E > 0.9 V, ORR and electrode oxide formation dynamics are interrelated phenomena and so, the system dynamics is more complex. In the case of Pt(111), it has been shown that ORR dynamics in this potential region may depend on the scan rate, the sweep direction and even the electrode rotation rate [19].

Figure 7 collects normalized voltammetric profiles for ORR on Pt(S)[*n*(111)x(111)] surfaces as well as the extrapolated Pt(111) curve, between 0.5 and 0.9 V, at 1600 rpm and 50 mV s^{-1}. As explained above, the extrapolated curve is built from intercepts to n = ∞ of linear plots of normalized current density at a fixed *E vs.* the step density. Due to small limiting current density variations with the meniscus height, current density values are normalized by the absolute value of the limiting current density, $|j_{lim}|$, for comparison. Additionally, because the sweep direction can play an important role in the shape of the CV [16, 19], only the positive going scan is shown. For clarity, inset to Fig. 7 depicts a detailed view of the ORR in the hydrogen adsorption/desorption region.

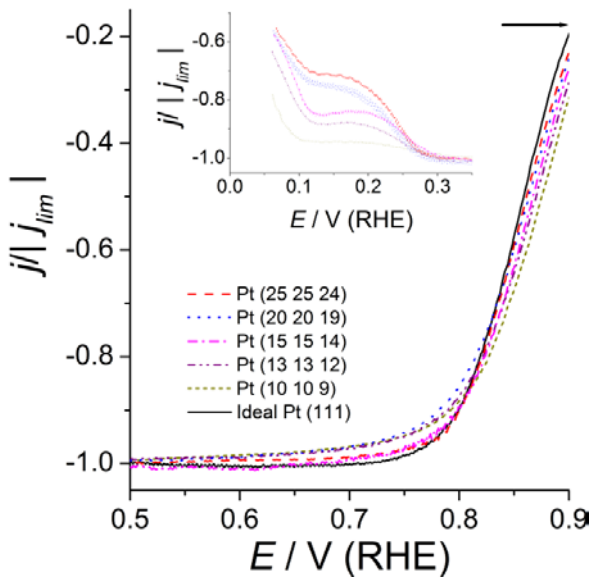

Fig. 7: Linear sweep voltammograms for oxygen reduction on the extrapolated Pt(111) and on experimental Pt(S)[*n*(111)x(111)] surfaces, in 0.1 M $HClO_4$. Curves are

normalized by the absolute value of j_{lim}. Rotation rate 1600 rpm and scan rate 50 mV s^{-1}. Inset: Detailed view of the hydrogen adsorption/desorption region.

Following the experimental results, the *ideal* ORR curve on Pt(111), calculated extrapolating experimental data from stepped surfaces with long terraces employed here, is less active for the ORR than all the stepped surfaces, in the pure kinetic region. The normalized kinetic current at 0.9 V and $E_{½}$ for the *ideal* ORR curve on Pt(111) are given in Fig. 6A and B, respectively (empty symbols). However, because the extrapolation is done at constant E, the $E_{½}$ value in the *ideal* curve, usually located in the mixed kinetic-transport controlled region, is higher than the intercept of the straight line in Fig. 6B, corresponding to n= ∞ but at constant current.

Nevertheless, if the *ideal* curve is compared to experimental results from previous works [15, 16, 19], the *ideal* ORR curve on Pt(111) is also less active than any experimental Pt(111) electrode reported, This is true even for those electrodes that do not apparently show any step contribution signal in the blank voltammogram, pointing out that a real electrode has always surface defects. Figure 8 depicts extrapolated and experimental ORR curves for Pt(111).

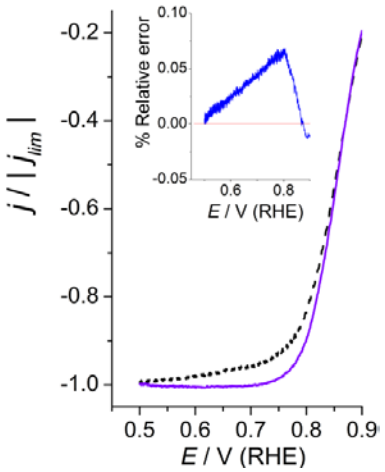

Figure 8: Extrapolated (solid) and experimental (dashed) ORR curves for Pt(111), in 0.1 M $HClO_4$ at 50 mV/s. Rotation rate 1600 rpm. Inset: Relative error percentage between extrapolated and experimental ORR curves.

In this respect, theoretical results, supposed to correspond to defect-free surfaces, should be compared to this *ideal* response, coming from extrapolation. However, as the relative error between experimental and extrapolated Pt(111) curves is lower than the error involved in most of theoretical predictions, the difference between these two curves would not hold much significance for theoretical studies at the present stage. Variations between curves in the transport-controlled region, ~0.6 to 0.8 V, in Figs. 7 and 8 are consequence of the mass transfer differences among electrodes due to the meniscus height on each measurement (see Fig. 5), and not because of the electron transfer kinetics.

3. Conclusions

In this work, the oxygen reduction reaction in acidic medium was measured on nano-structured stepped Pt(S)[*n*(111)x(111)] surfaces with the longest possible terraces widths, to determine the role of surface steps on the ORR activity and calculate an *ideal* ORR curve for a perfect, defect-free, Pt(111) surface. Results clearly show that increasing the surface step density linearly increases the electrode ORR activity, despite the higher oxygen and hydroxyl adsorption energies on stepped surfaces than on Pt(111). As expected, the *ideal* ORR curve for a defect-free Pt(111) surface, extrapolated from experimental data, has a lower electrocatalytic activity than experimental Pt(111) ORR activities reported in the present and previous works.

Acknowledgements

This work has been financially supported by a grant from COLCIENCIAS and the Universidad Nacional de Colombia in the framework of the National Program of Formation in Innovation Leaders (Contract No. 472 of 2007). Support from the Spanish

MICYNN though project CTQ2010–16271 and GV through PROMETEO/2009/045 (FEDER) are also greatly acknowledged.

References

1. A. J. Appleby, Catal. Rev. 4 (1970) 221–243.
2. S. Mukerjee, S. Srinivasan, M. P. Soriaga, J. McBreen, J. Electrochem. Soc. 142, (1995) 1409–1422.
3. J. Rossmeisl, A. Logadottir, J. K. Nørskov, Chem. Phys. 319 (2005) 178–184.
4. V. Viswanathan, H. A. Hansen, J. Rossmeisl, J. K. Nørskov, ACS Catal. 2 (2012) 1654–1660.
5. J. K. Nørskov, J. Rossmeisl, A. Logadottir, L. Lindqvist, J. Phys. Chem. B 108 (2004) 17886–.17892
6. Y. Okamoto and O. Sugino, J. Phys. Chem. C 114 (2010) 4473–4478.
7. M. T. M. Koper, J. Electroanal. Chem. 660 (2011) 254–260.
8. I. C. Man, H-Y Su, F. Calle-Vallejo, H. A. Hansen, J. I. Martinez, N. G. Inoglu, J. Kitchen, T. F. Jaramillo, J. K. Norskov, J. Rossmeisl, ChemCatChem. 3 (2011) 1159–1165.
9. J. Greeley, I. E. L. Stephens, A. S. Bondarenko, T. P. Johansson, H. A. Hansen, T. F. Jaramillo, J. Rossmeisl, I. Chorkendorff, J. K. Nørskov, N. Chem. 1 (2009) 552–556.
10. I. E. L. Stephens, A. S. Bondarenko, U. Grønbjerg, J. Rossmeisl, I. Chorkendorff, Energy Environ. Sci. 5 (2012) 6744–6762.
11. J. Greeley, J. Rossmeisl, A. Hellman, J. K. Nørskov, Z. Phys. Chem. 221 (2007) 1209–1220.

12. G. A. Tritsaris, J. Greeley, J. Rossmeisl, J. K. Nørskov, Catal Lett. 141 (2011) 909–913.

13. V. Viswanathan, F. Y.-F. Wang, Nanoscale 4 (2012) 5110–5117.

14. R. Rizo, E. Herrero, J.M. Feliu, Phys. Chem. Chem. Phys. 15 (2013) 15416–15425.

15. M. D. Maciá, J. M. Campiña, E. Herrero, J. M. Feliu, J. Electroanal. Chem. 564 (2004) 141–150.

16. A. Kuzume, E. Herrero, J. M. Feliu, J. Electroanal. Chem. 599 (2007) 333–343.

17. A. Hitotsuyanagi, M. Nakamura, N. Hoshi, Electrochim. Acta 82 (2012), 512–516.

18. F. J. Perez-Alonso, D. N. McCarthy, A. Nierhoff, P. Hernandez-Fernandez, C. Strebel, I. E. L. Stephens, J. H. Nielsen, I. Chorkendorff, Angew. Chem. Int. Ed. 51 (2012) 4641–4643.

19. A. M. Gómez–Marín, J. M. Feliu, ChemSusChem 6 (2013) 1091–1100.

20. A. Berná, V. Climent, J. M. Feliu, Electrochem. Commun. 9 (2007) 2789–2794.

21. A. M. Gómez-Marín, J. Clavilier, J. M. Feliu, J. Electroanal. Chem. 688 (2013) 360–370.

22. A. M. Gómez-Marín, J. M; Feliu, Electrochim. Acta 104 (2013) 367–377.

23. L. A. Kibler, A. Cuesta, M. Kleinert, D. M. Kolb, J. Electroanal. Chem. 484 (2000) 73–82.

24. J. Clavilier, D. Armand, S. Sun, M. Petit, J. Electroanal. Chem. 205 (1986) 267–277.

25. E. Herrero, J. M. Orts, A. Aldaz, J. M. Feliu, Surf. Sci. 440 (1999) 259–270.

26. J. Mostany, E. Herrero, J. M. Feliu, J. Lipkowski, J. Phys. Chem. B 106 (2002) 12787–12796.

27. J. Clavilier, A. Rodes, K. El Achi, M. A. Zamakhchari, J. Chim. Phys. 88 (1991) 1291–1337.

28. L. Cervera Gontard, L.-Y. Chang, C. J. D. Hetherington, A. I. Kirkland, D. Ozkaya, R. E. Dunin-Borkowski, Angew. Chem. Int. Ed. 46 (2007) 3683–3685.

29. L.-Y. Chang, A. S. Barnard, L. Cervera Gontard, R. E. Dunin-Borkowski, Nano Lett. 10 (2010) 3073–3076.

30. H. M. Villullas, M. López Tejeiro, J. Electroanal. Chem. 384 (1995) 25–30.

31. C. Korzeniewsky, V. Climent, J. M. Feliu, Electrochemistry at platinum single crystal electrodes. In: A. J. Bard and C. G. Zoski (Eds.), Electroanalytical Chemistry. A series of Advances, Vol. 24. CRC Press, 2012, pp. 75–170.

32. A. M. Gómez–Marín, J. M. Feliu, Cat. Sci. Tech. (2014) *Accepted*. DOI: 10.1039/c3cy01049j.

33. A. Björling, E. Herrero, J.M. Feliu, J. Phys. Chem. C 115 (2011) 15509–15515.

34. M. J. T. C. van der Niet, N. Garcia-Araez, J. Hernandez, J. M Feliu, M. T. M. Koper, Cat. Today, 202 (2013) 105–113.

35. N. M. Markovic, R. R. Adzic, B. D. Cahan, E. B. Yeager, J. Electroanal. Chem. 377 (1994) 249–259.

36. F. Tian, A. B. Anderson, J. Phys. Chem. C 115 (2011) 4076–4088.